

Half-metallic Antiferromagnet BaCrFeAs₂

Shu-Jun Hu and Xiao Hu

World Premier International Center for Materials Nanoarchitectonics (MANA)

National Institute for Materials Science, Tsukuba 305-0044, Japan

(Dated: June 21, 2021)

First-principles calculations and a tight-binding analysis predict that the iron-pnictide BaCrFeAs₂ is a promising candidate for half-metallic material with fully-compensated magnetization. The transition-metal ions Cr and Fe prefer the three-dimensional intervening lattice, which yields the antiferromagnetic order of spin orientations. Due to the difference between Cr and Fe in the electronegativity, a band gap is opened at the Fermi level in the spin channel in which Fe provides the majority carriers. The selective hybridization between 3d orbitals of Cr and As:4p states due to the peculiar lattice structure of the iron-pnictide is shown to be crucial for the novel properties.

I. INTRODUCTION

As one of the elements well explored from the ancient time, iron (Fe) had not been a central player in the modern electronic technologies. However, the recent discovery of superconductivity in iron-pnictide materials [1] certainly has opened a new chapter of study on Fe. The parent iron-pnictide materials are metallic and antiferromagnetic (AFM), and superconductivity is realized by carrier doping [1] or application of pressure [2]. So far the main focus on the iron-pnictide materials has been superconductivity, and the AFM order is to be suppressed as a competitor. However, it has been revealed during the investigation of the mechanism of superconductivity that the AFM order of Fe ions itself is also of interest which is established by the peculiar lattice structure of iron-pnictides via the ferro-orbital ordering [3]. It will be fantastic if one can successfully explore the possibility of iron-pnictides as a platform for novel spin-dependent transport properties in which the magnetic order plays a direct role.

Of many possibilities, we focus here on a novel class of materials called half-metallic antiferromagnet (HMAFM), which is metallic in one spin channel and exhibits a gap at the Fermi level, thus insulating, in the other spin channel while showing zero total magnetization in a unit cell [4]. HMAFM can generate spin-polarized current without perturbing the surrounding elements magnetically in a device, and thus is particularly useful in spintronics applications. HMAFM can also be the parent material for single spin superconductivity with triplet Cooper pairs due to the finite density of states in only one spin channel [5]. Since the first proposal [4], the possibility of HMAFM has been investigated primarily in Heulser alloys [6, 7] and double perovskites [8–14]. The transition-metal (TM) chalcogenide superlattice [15], thiospinels [16] and some disordered systems, such as diluted magnetic semiconductors [17, 18], vacancy-induced TM oxides [19] and hole-doped cuprates [20] are also predicted to be the possible candidates. Up to date, it is still lacking of a definite confirmation of such novel material.

It is intriguing to notice that the iron-pnictide mate-

rials can be good candidates for HMAFM. The ground state of these materials is AFM and poorly metallic. In order to achieve the HMAFM, one only needs to open a gap in one spin channel while keeping the AFM order with compensated magnetization. In the simplest picture, a Fe atom has six 3d electrons and shows an effective spin moment of $4 \mu_B$ due to the intra-atomic Hund's coupling. In order to achieve HMAFM, one can choose the Chromium (Cr) atom to substitute half of the Fe atoms since Cr possesses four 3d electrons. It is expected that the Cr atom will not change the AFM order of compensated magnetization of the parent material, while modify the band structure due to the different atomic number from Fe.

In the present work, we focus on a typical iron-pnictide BaFe₂As₂ [21], which belongs to the so-called '122' family. Among the well-studied iron-pnictides, the '122' family has the shortest As-As bond along the c axis, which enhances the interlayer coupling. From first-principles calculations on the electronic structure of BaCrFeAs₂, it is revealed that (i) Cr and Fe ions prefer a three-dimensional (3D) intervening lattice; (ii) the magnetic

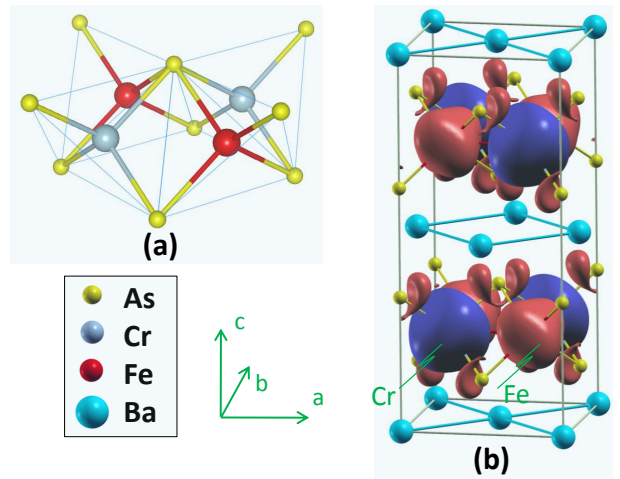


FIG. 1. (a) Crystal structure of the TM-As layer of BaCrFeAs₂; (b) Spin-density of the AFM state (blue/red surface: spin-up/spin-down). Isovalue= $0.025 e/\text{\AA}^3$.

moments of Cr and Fe ions are aligned antiferromagnetically, and with small but non-negligible contributions from As atoms parallel to that from Fe ions, the total spin magnetization in a unit cell is zero; (iii) a gap is opened at the Fermi level (E_F) in the spin channel where Fe electrons contribute as majority carriers by the hybridization between As:4p states and minority Cr:3d states due to the difference in the electronegativity between Fe and Cr as well as the peculiar crystal structure of iron-pnictide. Based on these results, we predict BaCrFeAs₂ as a possible HMAFM.

This paper is organized as follows. In the next section the computational details of calculations are briefly described. In the first part of section III, we focus on the electronic structure of BaCrFeAs₂; then a tight-binding (TB) picture is presented. Finally the summary of the paper is given in section IV.

II. COMPUTATIONAL DETAILS

First-principles calculations were performed by VASP package [22, 23] within the scheme of PAW method [24] and generalized gradient approximation [25] for the exchange-correlation functional [26]. $8 \times 8 \times 4$ Monkhorst-Pack special points and 500 eV are used for k sampling and plane-wave basis set. Starting from the experimental lattice parameters of BaFe₂As₂ in tetragonal structure [27], both the ion coordinations and lattice parameters are fully relaxed until the force and stress are less than 0.01 eV/Å and 1 kBar. Calculations were also performed by the Quantum-Espresso package [28], and a good agreement is achieved.

The on-site energies and hopping integrals of the TB model are calculated by the maximally localized Wannier functions (MLWF) method as implemented in the Wannier90 package [29] jointly with Quantum-Espresso [28]. The Bloch wavefunction of BaCrFeAs₂ is first calculated in density functional formalism. By specifying the 3d orbitals of TM ions and 4p orbitals of As ions as the initial guess, the periodic wavefunctions are transformed to the MLWF representation in real space. Meanwhile, the on-site energies and hopping integrals can be obtained. It is noticed that the TB model including only the nearest neighboring hoppings can reproduce well the DFT band structures.

III. RESULTS AND DISCUSSION

A. First-principles results

In BaFe₂As₂, Fe ions tetrahedrally coordinated by As atoms form Fe-As layers, which are sandwiched by Ba layers. We concentrate on the situation that half of the Fe atoms are substituted by Cr atoms in a $\sqrt{2} \times \sqrt{2} \times 1$ cell. The possible atomic configurations which have been studied include: (1) cross-checkerboard type as shown in

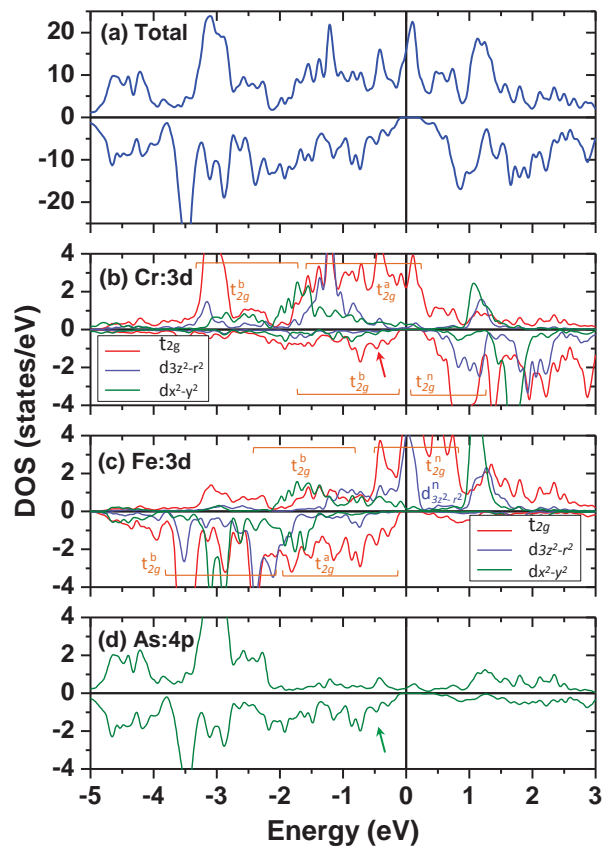


FIG. 2. (a) Total density of states (DOS) of half-metallic antiferromagnet BaCrFeAs₂. (b) and (c) Projected DOS of 3d states for Cr and Fe, respectively. The Fermi energy E_F is set to energy zero. The bonding, anti-bonding and non-bonding states of t_{2g} are labeled as t_{2g}^b , t_{2g}^a and t_{2g}^n , respectively. (d) Projected DOS of As:4p states.

Figure 1b, (2) checkerboard type with same positions of Cr and Fe ions along c axis, (3) alternating Cr and Fe layers, and (4) alternating Cr and Fe stripes along a or b axis. We calculate the total energies of them with all the possible spin orderings of the TM ions. It is revealed that the ground state of BaCrFeAs₂ is characterized by the intervening Fe and Cr ions and 3D AFM spin order, as shown in Figure 1b. The resultant lattice parameters of $a=5.725$ Å and $c=13.290$ Å are in good agreement with the experiments [30].

The magnetization is mainly contributed by Fe ($-2.62 \mu_B$) and Cr ($2.75 \mu_B$) ions. In addition, each As atom carries a small magnetic moment ($-0.08 \mu_B$) parallel to that of Fe ions due to the hybridization between As:4p and TM:3d electrons. The Ba layers act as charge reservoir, and thus the magnetic moment of Ba²⁺ ions is negligible. According to the calculation, the magnetic moments of the Fe, Cr and As atoms compensate completely, resulting in the total magnetization of $0.0 \mu_B$ per unit cell.

The total density of states (DOS) of BaCrFeAs₂ is depicted in Figure 2a. While the spin-up channel exhibits an evident metallic character similar with the parent ma-

terial [31], a gap of ~ 0.3 eV emerges at E_F in the spin-down channel. Combining the zero magnetization and half-metallic band structure, BaCrFeAs_2 is expected to be a HMAFM.

Let us look into the detailed electronic band structure of the new material BaCrFeAs_2 . In the spin-up channel, Cr nominally has four 3d electrons, and thus its majority 3d band is not fully occupied, as illustrated by Figure 2b. The hybridization between As:4p and Cr: t_{2g} states forms the bonding states (t_{2g}^b) deep in the valence band, and partially occupied anti-bonding states (t_{2g}^a) around E_F . Although there exist Fe:3d-As:4p as well as Fe: $3d_{x^2-y^2}$ -Cr: $3d_{x^2-y^2}$ hybridizations, most of the Fe:3d minority states remain non-bonding and locate around E_F (t_{2g}^n and $d_{3z^2-r^2}^n$ in Figure 2c). BaCrFeAs_2 is therefore metallic in the spin-up channel.

In the spin-down channel, Fe:3d majority states lie deeply in the valence band and are fully occupied, as shown in Figure 2c. Most of the minority states of Cr are above E_F and form the bottom of conduction band, in contrast with Fe in the spin-up channel, due to the difference in the electronegativity between Cr and Fe. Around the top of valence band there are noticeable contributions from Cr:3d minority states as indicated in Figure 2b. It is intriguing to notice that the lattice structure of the present iron-pnictide material is crucial for opening a gap of ~ 0.3 eV between Cr:3d states in the spin-down channel. Since the Cr: $3d_{xy}$ orbitals reside on the TM plane with their petals pointing to the nearest neighboring Cr ions along (110) or (1-10) direction, and the As atoms just locate above the center of the TM squares (see inset of Figure 3a), the As: $4p_z$ orbitals mediate the exchange interaction between the Cr: $3d_{xy}$ states. Meanwhile, the As: $4p_y$ (As: $4p_x$) state provides an evident bridge for the exchange coupling between the two Cr: $3d_{xz}$ (Cr: $3d_{yz}$) states. As the result, the spin-down As:4p states in the vicinity of E_F hybridize with a part

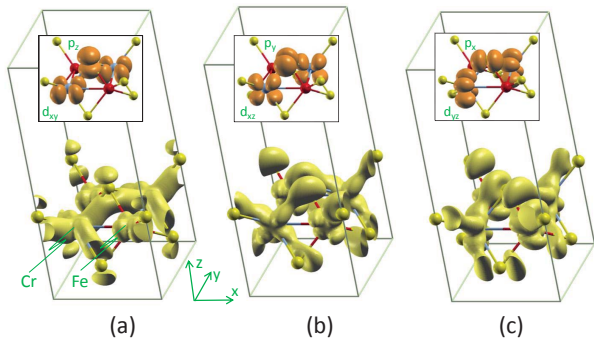


FIG. 3. Band-decomposed charge density for the (a) Cr: $3d_{xy}$ bonding via As: $4p_z$, (b) Cr: $3d_{xz}$ bonding via As: $4p_y$ and (c) Cr: $3d_{yz}$ bonding via As: $4p_x$ at the Γ point of the spin-down valence band maximum associated with a $\sqrt{2} \times \sqrt{2} \times 1$ cell. Only one TM-As layer is shown. Isovalue=0.004 $e/\text{\AA}^3$ for (a) and 0.008 $e/\text{\AA}^3$ for (b) and (c). Insets schematically show the corresponding atomic orbitals of Cr and As.

TABLE I. Hopping integrals between the orbitals of nearest-neighboring As-As, As-Cr/Fe and Cr-Fe ions derived from the MLWF calculation in the units of eV ^a

orbitals	hopping integrals	
	Spin-up	Spin-down
As: p_x/p_y -Cr: d_{yz}/d_{xz}	0.70	0.80
As: p_z -Cr: d_{xy}	0.61	0.68
As: p_x/p_y -Cr: $d_{x^2-y^2}$	0.50	0.65
As: p_z -Cr: $d_{3z^2-r^2}$	0.50	0.65
As: p_x/p_y -Cr/Fe: $d_{3z^2-r^2}$	0.24	0.27
As: p_x/p_y -Fe: d_{yz}/d_{xz}	0.66	0.58
As: p_z -Fe: d_{xy}	0.57	0.50
As: p_x/p_y -Fe: $d_{x^2-y^2}$	0.50	0.39
As: p_x/p_y -As: p_x/p_y (I)	0.27	0.27
As: p_x -As: p_y (I)	0.34	0.33
As: p_z -As: p_z (II)	0.29	0.28
As: p_z -As: p_x/p_y (II)	0.41	0.38
As: p_x/p_y -As: p_x/p_y (II)	0.34	0.30
As: p_z -As: p_z (III)	0.73	0.76
Cr/Fe: $d_{x^2-y^2}$ -Fe/Cr: $d_{3z^2-r^2}$	0.22	0.21
Cr: d_{xz}/d_{yz} -Fe: d_{xz}/d_{yz}	0.28	0.28
Cr: $d_{x^2-y^2}$ -Fe: $d_{x^2-y^2}$	0.37	0.37
Cr: d_{xy} -Fe: d_{xy}	0.27	0.26

^a The Roman numbers denote the hoppings between As-As ions (I) within the same As plane, (II) crossing the TM plane and (III) along the c axis, which can be read from Figure 1.

TABLE II. Onsite energy of As:4p and TM:3d orbitals for the TB model derived from the MLWF calculation in the units of eV

	Cr: $d_{3z^2-r^2}$	Cr: d_{xz}/d_{yz}	Cr: $d_{x^2-y^2}$	Cr: d_{xy}
Spin up	-1.61	-1.08	-1.62	-1.38
Spin down	0.18	0.61	0.20	0.65
	Fe: $d_{3z^2-r^2}$	Fe: d_{xz}/d_{yz}	Fe: $d_{x^2-y^2}$	Fe: d_{xy}
Spin up	-0.24	-0.17	-0.46	-0.14
Spin down	-2.66	-1.96	-2.71	-2.00
	As: p_z	As: p_x/p_y		
Spin up	-2.24	-2.39		
Spin down	-2.23	-2.34		

of the Cr: t_{2g} minority states (Figure 2b and 2d), and lower their energies to the valence band. These features are well captured by the band-decomposed charge density [22, 23] depicted in Figure 3 obtained by calculations based on the $\sqrt{2} \times \sqrt{2} \times 1$ cell.

B. Tight-binding Model

For a better understanding on the novel HMAFM property of BaCrFeAs_2 , in which many orbitals contribute around E_F , it is helpful to build a TB picture. For this purpose, we adopt the MLWF method [28, 29], which

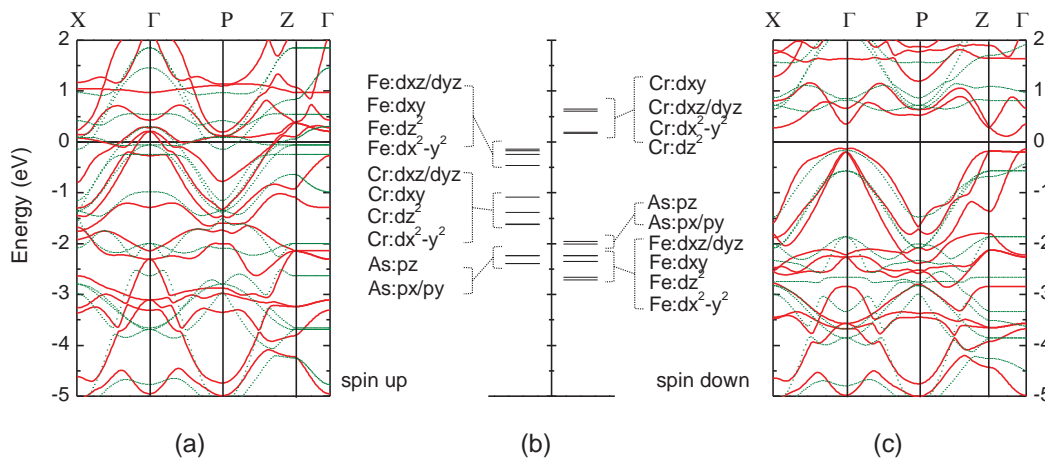


FIG. 4. Band structures of BaCrFeAs₂ with the red solid and green dotted curves denote results based on the first-principles calculations and the TB model, respectively. (a)/(c) for spin-up/down channel; (b) for on-site energies of relevant orbitals of the TB model derived from the MLWF calculation.

yields both on-site energies and hopping integrals of the TB model. Since the whole TM:3d and As:4p orbitals are involved in the covalency, all of them are treated as the initial guess for orbital projections. It is confirmed that the DFT results can be perfectly reproduced. We then reduce the hopping ranges to the minimum with which one can still capture the main features of the DFT results. In this way, the important orbitals which govern the band dispersion around E_F are identified as TM: t_{2g} and As:4p, and the hopping integrals are for the nearest neighbors only.

The numerical results for the hopping integrals and the on-site energies are given in Table I and II respectively, and the band structures derived from the TB model are shown in Figure 4 in fairly good agreement with the VASP results. The onsite energies of spin-up Fe:3d states are slightly below E_F , while the spin-down Cr:3d orbitals are slightly higher than E_F . It is clear that this difference is responsible for the half metallic feature of the present material BaCrFeAs₂.

As listed in Table I, the As: p_z -As: p_z hopping along c axis is quite large (~ 0.7 eV) due to the crystal structure of the present '122' system with the shortest As-As bond along the c axis. This interaction is crucial for the c axis AFM order of BaCrFeAs₂, and thus the feature of HMAFM, in contrast to the case of the so-called '1111' system [32]. Therefore we predict that the present BaCrFeAs₂ as well as other '122' materials are the most promising candidates for HMAFM among the

iron-pnictides.

IV. CONCLUSIONS

To summarize, based on first-principles calculations and a TB model we predict that BaCrFeAs₂ is a candidate material for half-metallic antiferromagnet. The novel half-metallic band structure of this material is generated by the selective, strong hybridization between As:4p states and minority Cr:3d states, due to the difference in the electronegativity between Fe and Cr. Both the density-functional calculations and the TB analysis reveal clearly that the crystal structure of iron-pnictide is crucial for opening a gap around E_F as large as ~ 0.3 eV in the single spin channel. The zero magnetization is achieved by the magnetic compensation of Cr, Fe and As atoms. It is highly anticipated that the theoretical prediction formulated in the present work can be checked experimentally. The endeavor will then open a new field of iron-based spintronics.

ACKNOWLEDGMENTS

The authors thank I. V. Solovyev, B. Liu and Y.-M. Nie for discussions. The calculations were performed on Numerical Materials Simulator (SGI Altix) of NIMS. This work was supported by WPI Initiative on Materials Nanoarchitronics, MEXT, Japan.

- [1] Y. Kamihara, T. Watanabe, M. Hirano, and H. Hosono, *J. Am. Chem. Soc.* **130**, 3296 (2008).
 [2] M. S. Torikachvili, S. L. Bud'ko, N. Ni, and P. C. Canfield, *Phys. Rev. Lett.* **101**, 057006 (2008).

- [3] C.-C. Lee, W.-G. Yin, and W. Ku, *Phys. Rev. Lett.* **103**, 267001 (2009).
 [4] H. van Leuken and R. A. de Groot, *Phys. Rev. Lett.* **74**, 1171 (1995).

- [5] W. E. Pickett, Phys. Rev. Lett. **77**, 3185 (1996).
- [6] S. Wurmehl, H. C. Kandpal, G. H. Fecher, and C. Felser, J. Phys.: Condens. Matter **18**, 6171 (2006).
- [7] I. Galanakis, K. Özdoğan, E. Şaşoğlu, and B. Aktas, Phys. Rev. B **75**, 172405 (2007).
- [8] W. E. Pickett, Phys. Rev. B **57**, 10613 (1998).
- [9] J. H. Park, S. K. Kwon, and B. I. Min, Phys. Rev. B **65**, 174401 (2002).
- [10] M. S. Park and B. I. Min, Phys. Rev. B **71**, 052405 (2005).
- [11] Y. K. Wang and G. Y. Guo, Phys. Rev. B **73**, 064424 (2006).
- [12] M. Uehara, M. Yamada, and Y. Kimishima, Solid State Commun. **129**, 385 (2004).
- [13] Y. K. Wang, P. H. Lee, and G. Y. Guo, Phys. Rev. B **80**, 224418 (2009).
- [14] V. Pardo and W. E. Pickett, Phys. Rev. B **80**, 054415 (2009).
- [15] M. Nakao, Phys. Rev. B **77**, 134414 (2008).
- [16] M. S. Park, S. K. Kwon, and B. I. Min, Phys. Rev. B **64**, 100403(R) (2001).
- [17] H. Akai and M. Ogura, Phys. Rev. Lett. **97**, 026401 (2006).
- [18] L. Bergqvist and P. H. Dederichs, J. Phys.: Condens. Matter **19**, 216220 (2007).
- [19] D. Ködderitzsch, W. Hergert, Z. Szotek, and W. M. Temmerman, Phys. Rev. B **68**, 125114 (2003).
- [20] Y.-M. Nie and X. Hu, Phys. Rev. Lett. **100**, 117203 (2008).
- [21] M. Rotter, M. Tegel, D. Johrendt, I. Schellenberg, W. Hermes, and R. Pöttgen, Phys. Rev. B **78**, 020503(R) (2008).
- [22] G. Kresse and J. Hafner, Phys. Rev. B **47**, 558 (1993).
- [23] G. Kresse and J. Furthmüller, Phys. Rev. B **54**, 11169 (1996).
- [24] P. E. Blöchl, Phys. Rev. B **50**, 17953 (1994).
- [25] J. P. Perdew, K. Burke, and M. Ernzerhof, Phys. Rev. Lett. **77**, 3865 (1996).
- [26] It is widely accepted that the electronic structure of ironpnictides (particularly the Fermi surface) predicted by the local density approximation (LDA) or GGA is in good agreement with the ARPES experiments. In the current study we focus on the half-metallic bands in the vicinity of the Fermi level. It is expected that GGA can predict the accurate band structures of BaCrFeAs₂ and therefore the strong correlation effect (Hubbard U) is unnecessary.
- [27] Q. Huang, Y. Qiu, W. Bao, M. A. Green, J. W. Lynn, Y. C. Gasparovic, T. Wu, G. Wu, and X. H. Chen, Phys. Rev. Lett. **101**, 257003 (2008).
- [28] <http://www.quantum-espresso.org>.
- [29] A. A. Mostofi, J. R. Yates, Y.-S. Lee, I. Souza, D. Vanderbilt, and N. Marzari, Comput. Phys. Commun. **178**, 685 (2008).
- [30] A. S. Sefat, D. J. Singh, L. H. VanBebber, Y. Mozharivskyj, M. A. McGuire, R. Jin, B. C. Sales, V. Keppens, and D. Mandrus, Phys. Rev. B **79**, 224524 (2009).
- [31] D. J. Singh, Phys. Rev. B **78**, 094511 (2008).
- [32] M. Nakao, J. Phys.: Conf. Ser. **150**, 052182 (2009).